SEISMOTECTONICS OF SIERRA PIE DE PALO, A BASEMENT BLOCK UPLIFT IN THE ANDEAN FORELAND OF ARGENTINA

By Marc Regnier, Jean Luc Chatelain, Robert Smalley, Jr., Jer-Ming Chiu, Bryan L. Isacks, and Mario Araujo

ABSTRACT

We operated a digitally recording seismic network from September 1987 to May 1988 in the San Juan Province of northwestern Argentina. The network was located in the thin-skinned Precordillera and thick-skinned Sierras Pampeanas tectonic provinces of the Andean foreland. Our data provide a detailed view of the crustal seismicity of Sierra Pie de Palo, one of the most seismically active mountain blocks of the Sierra Pampeanas and the site of the destructive M_s 7.3 Caucete earthquake in 1977. Most of the well-located shallow earthquakes we recorded occurred directly beneath the range between 9 and 30 km depth, with a maximum activity around 25 km depth. The morphology of the range, seismicity pattern, and focal mechanisms strongly suggest Sierra Pie de Palo is cut into two blocks by a northeast-southwest striking fracture. In the northern block, seismicity occurs along a well-defined west-dipping seismic zone, while the southern block is characterized by east-dipping seismic layers. Both dipping zones connect to a subhorizontal mid-crustal detachment that we interpret as the lower boundary of the brittle failure domain. The complex fault geometry and large variety of focal mechanism orientations we observe suggest that the ongoing seismic activity is a continuation of the aftershock sequence of the 1977 Caucete earthquake. We therefore interpret the two principal dipping zones to be buried thrusts activated during the complex rupture of the 1977 earthquake. Inversion of the focal mechanism data for the orientation of the regional deviatoric stress tensor shows the maximum compressive stress, σ_1, oriented at an azimuth of N107°E. This direction is approximately orthogonal to the trend of the Sierra but rotated 27° clockwise with respect to the current Nazca-South America convergence direction. This result suggests that local boundary effects within the Sierras Pampeanas Province partially control the shortening direction in the crust. It may also indicate that a component of sinistral strike-slip motion exits within the Precordillera to the west of the Sierras Pampeanas.

INTRODUCTION

The Andes have long been considered the archetypal example of mountain building by subduction-driven magmatic addition to the crust. Recent studies, however, propose models in which a crustal thickening due to shortening across the orogen is the principal mountain building process (Isacks, 1988). An important contribution to this evolution of ideas was the recognition of along-strike segmentation of the two plates that correlate temporally and spatially. In the Nazca Plate, segmentation is manifested by variations in subduction angle (Stauder, 1973, 1975; Baranzangi and Isacks, 1976, 1979; Isacks and Baranzangi, 1977), while in the upper plate tectonic style varies (Jordan et al., 1983, Jordan and Allmendinger, 1986; Sébrier et al., 1985). In segments where the underlying plate subducts at steep dip angles (approximately 30°), e.g., under the Altiplano-Puna plateau, deformation of the overlying plate is restricted to

the primary mountain belt. In segments of flat subduction, e.g., central Chile/western Argentina, deformation continues toward the craton beyond the foreland thrust belt. This is unusual, as the thin-skinned foreland thrust belt is typically the cratonwardmost part of a mountain belt. The Sierras Pampeanas Province, between 26°S and 33°S and 63°W and 68.5°W (Figure 1), is in a region over flat subduction, cratonward (east) of the thin-skinned Precordillera thrust belt, and the easternmost tectonic province of the Andean orogen. In the regions over flat subduction active crustal seismicity to 40 km depth, focal mechanisms of crustal earthquakes and geologic evidence support models in which the mountain building is due to compression and the resulting crustal shortening (Dorbath et al., 1986; Langer and Bollinger, 1988; Suarez et al., 1990; Smalley and Isacks, 1990).

    Isacks (1988) proposed a model for uplift of the Altiplano-Puna and the main Andean Cordillera over a 30°-dipping segment of the subducted plate based on crustal thickening due to shortening of a ductile lower crust rather than magmatic intrusion. In this model, most of the thickening occurs beneath the Principal Cordillera. In the regions of flat subduction, however, absence of a high plateau and the significant amounts of deformation east of the foreland thrust belt suggest a different mode of crustal thickening. Estimation of the amount and direction of crustal shortening in the Sierras Pampeanas is crucial for understanding the along-strike differences in mountain building process in the Andean orogen. The issues to be discussed here are (1) to what extent the whole Sierras Pampeanas Province, rather than just the crust beneath the mountain blocks, is affected by crustal deformation and shortening, and (2) what the depth range is over which this crustal deformation occurs through brittle failure rather than ductile processes. To define the active fault geometry and constrain the uplift mechanism of the Sierras Pampeanas, a dense digitally recording portable seismic network was deployed in San Juan, Argentina (Fig. 2) for 9 months in 1987 and 1988. This paper presents our results concerning active deformation of Sierra Pie de Palo, one of the Sierras Pampeanas mountain blocks. Sierra Pie de Palo has been the site of several large historical earthquakes, most notably the M_s 7.3 Caucete earthquake in 1977. A re-interpretation of the rupture history of this large event that closely matches the resolved fault system is also proposed.

TECTONIC SETTING

    The Sierras Pampeanas are basement block uplifts of metamorphosed Precambrian crystalline rock (Caminos et al., 1982) bounded by large, generally north–south-trending thrust or reverse faults and separated by shallow intermontane valleys filled with relatively undeformed Carboniferous and younger sediments (Salfity and Gorustovich, 1983). Available focal mechanism solutions of large earthquakes in the Sierras Pampeanas and neighboring tectonic provinces (Stauder, 1973; Chinn and Isacks, 1983) indicate mostly reverse faulting on north–south-striking faults, which agrees with mapped surface faults and large scale mountain structures. The focal mechanism data support models with a regional east–west compressive stress regime produced by convergence of the Nazca plate beneath the western margin of the South America plate.

    Sierra Pie de Palo is an 80-km-long, north-northeast-trending, elliptically shaped mountain range with 3 km of topographic relief situated 30 km east of
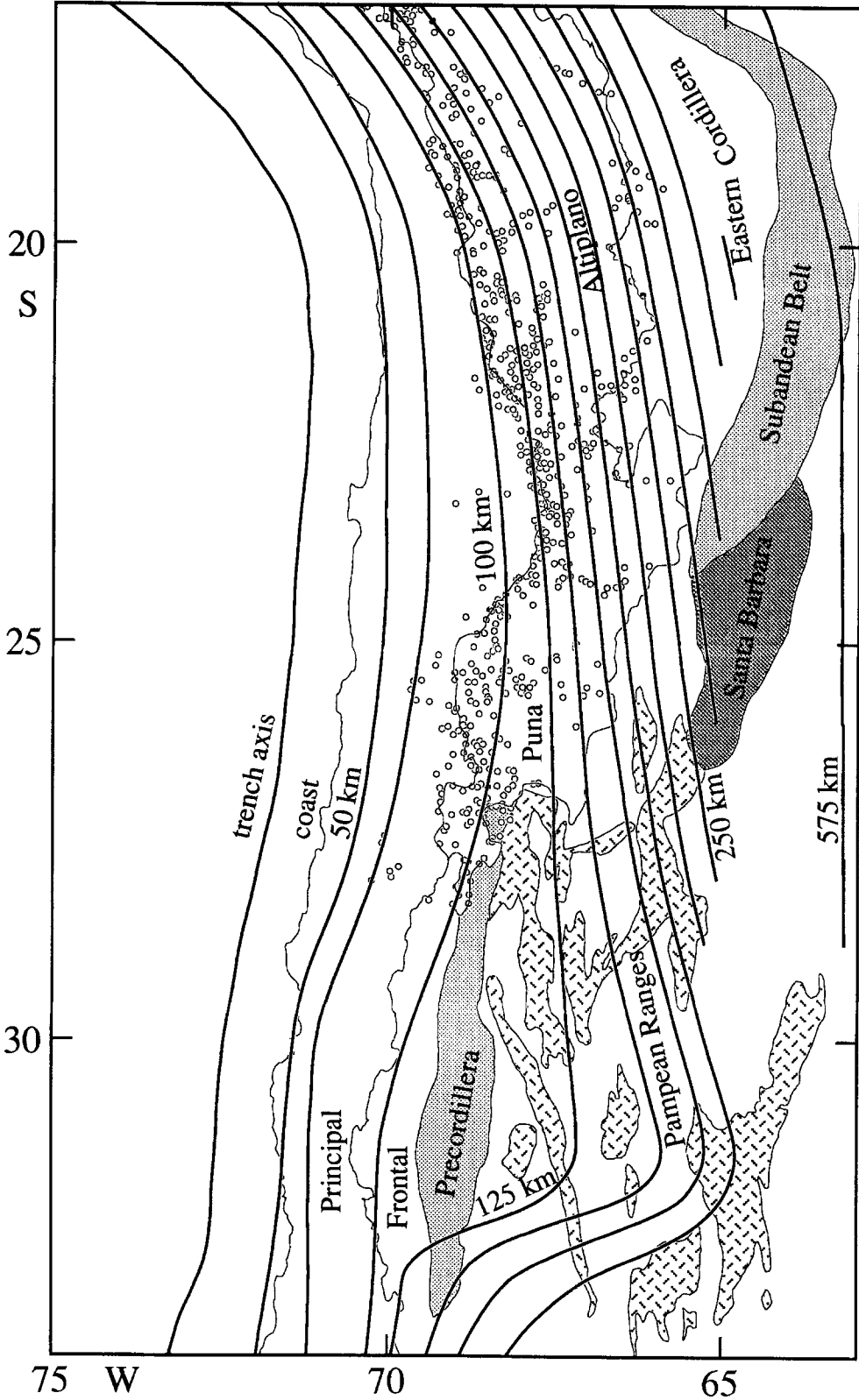
FIG. 1. Map of western South America illustrating upper plate tectonic features, volcanic arc, and contours of the Wadati-Benioff zone (WBZ). Along-strike segmentation of the upper plate tectonic provinces correlates with the along-strike segmentation of the WBZ (Jordan et al., 1983). The distribution of Neogene volcanos (open circles) (Isacks, 1988) shows an active magmatic arc over the steep WBZ segment and the absence of an active arc over the flat segment.
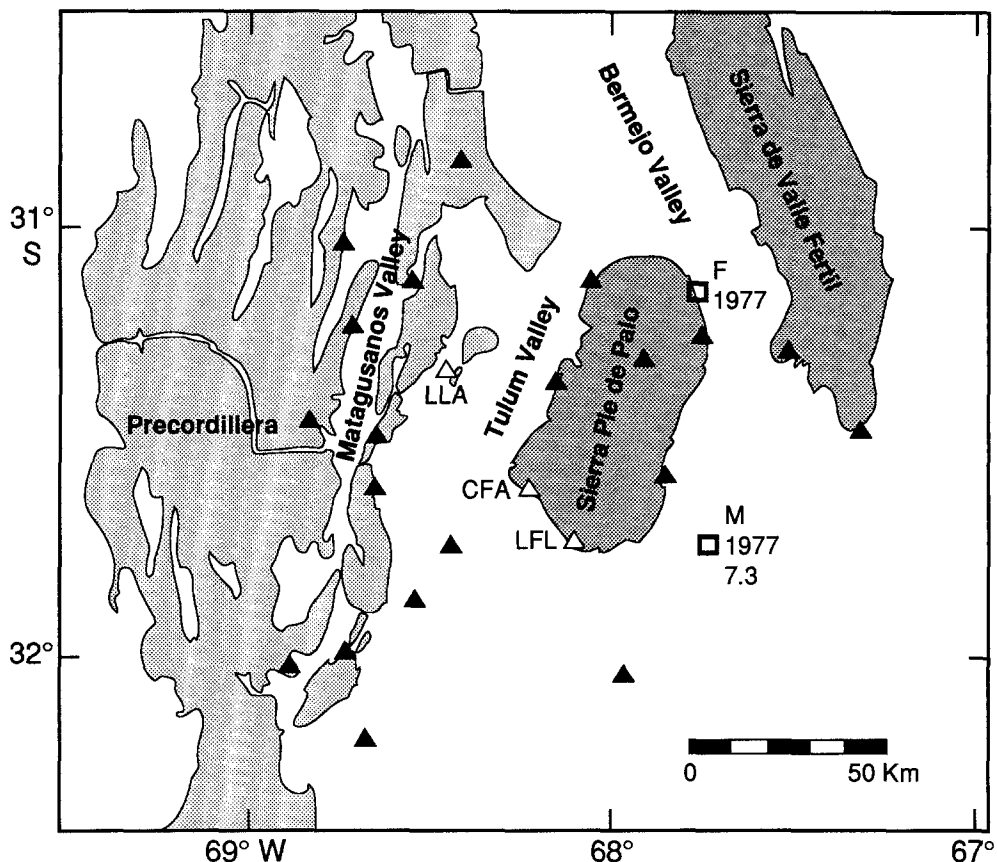
FIG. 2. Map of San Juan region. Mountain ranges are shaded light for the sedimentary rocks of the thin-skinned Precordillera and dark for the basement block uplifts of the Sierras Pampeanas. Intermontane valleys of Carboniferous to Quaternary sediments are shown in white. The Eastern Precordillera is the chain of mountains east of the Matagusanos Valley. The seismic network stations are shown by solid triangles for the three-component high-gain/low-gain stations and open triangles for the small aperture arrays composed of multiple three-component high-gain/low-gain or high-gain/low-gain stations. Epicenters of the 1977 foreshock (F) and Mainshock (M) are also shown (dated open squares; Chinn and Isacks, 1983; Kadinsky-Cade, 1985).

the Precordillera. It is composed of metamorphic rocks that indicate the exposed crust was buried to a depth of 20 to 35 km in the late Precambrian (Jordan and Allmendinger, 1986). A high level of crustal seismic activity is associated with Sierra Pie de Palo, with event depths ranging from 10 to 30 km (Smalley and Isacks, 1990; Regnier et al., 1988). This activity includes the Caucete earthquake, which has been studied through analysis of focal mechanisms, synthetic seismogram modeling, a local aftershock survey, and leveling data from the epicentral area. The earthquake has been interpreted as a complex event that occurred beneath the range with a hypocenter at 17-km depth on a west-dipping fault that ruptured down-dip (Chinn and Isacks, 1983; Kadinsky-Cade, 1985) or alternately with a hypocenter at 25 km depth on an east-dipping fault that ruptured up-dip (Langer and Bollinger, 1988).

To the west of Sierra Pie de Palo, the contact between the Precambrian basement of the Sierras Pampeanas Province and the basement of the Precordillera Province is covered by sediments of the Tulum Valley. Crustal seis-

micity in the vicinity of the boundary region, while not as active as beneath Sierra Pie de Palo, reaches depths of 35 km (Smalley and Isacks, 1990; Smalley et al., 1992) and indicates that the basement deformation is also found beneath the thin-skinned Precordillera.

DATA ACQUISITION

A portable, digitally recording seismic network of three-component stations (PANDA, Chiu et al., 1991) was operated in the San Juan area from September 1987 to May 1988 and covered an area of roughly 150 km north-south by 100 km east-west (Fig. 2). The network consisted of 26 sites, three of which (CFA, LFL, and LLA) contained small aperture (several meters to 1 km) multi-station arrays (six to 11 three-component stations). Approximately 75 events were recorded per day producing a total of over 20,000 earthquakes. Our study concentrates on the period of November 1987 to April 1988. This period contains two thirds to three quarters of the total data set and covers the time during which the complete network was operational. Initial processing included grading the events based on the number of well-recorded P arrivals (A for events with well-recorded arrivals through the whole network, B for events where a few stations did not have well-recorded arrivals, and C for events with down to six or seven well-recorded arrivals). All A and B quality events from the Sierra Pie de Palo region, and C events from a 3-week period around an m_b 5.3 event beneath Sierra Pie de Palo, were selected for this study. P arrival times were read using an interactive seismic processing program with a precision of one or two digital samples (i.e., 0.01 to 0.02 sec). S arrivals were picked from the horizontal components and verified on horizontal components rotated to the backazimuth after preliminary location. This eliminated the possibility of confusing S-to-P converted wave arrivals with S. The precision of the S arrival times is between 0.05 and 0.1 sec, which is one half to one cycle at the predominant 10- to 15-Hz frequency of the S waves. The network used FM telemetry to transmit the data in real time to a recording center where it was digitized with a common time base, so interstation timing was not a problem.

Initial locations were obtained using HYPOINVERSE (Klein, 1978) and a three-layer velocity model (Table 1) modified from the four-layer model of Bollinger and Langer (1988). The top two layers of the Bollinger and Langer velocity model were derived from shallow refraction surveys in the sedimentary

TABLE 1

CRUSTAL VELOCITY MODELS

Three Layers Over Half-Space Model	
Depth (km)	Velocity (km/sec)
0.0	5.88
10.0	6.20
32.0	7.30
45.0	8.10

Three-layers models from INPRES; the top layer of the velocity model is based on shallow refraction data (Bollinger and Langer, 1988) and the bottom two layers from regional earthquake studies (Volponi, 1968).

basins around Sierra Pie de Palo (YPF, unpublished data). We did not use the top unconsolidated sediment layer, because most of our stations were on out-crops of Precambrian metamorphic crystalline rock or competent sedimentary rock. Both P and S were used for locating the earthquakes with a Vp/Vs of 1.75 obtained from a least-squares fit of a line on Wadati diagrams (Vlasity, 1988). Locations of the events beneath Sierra Pie de Palo are largely determined by the subset of stations on and close to Sierra Pie de Palo. This removes the distinction between A, B, and C events since almost all selected events have well-recorded P and S arrivals at the stations of this subset. Average RMS residuals of approximately 0.3 sec were found for our three-layer velocity model or slight variations of it. Final locations were obtained using joint hypocentral determination, JHD (Frohlich, 1979), which reduced the average RMS residual of the 620-event data set to 0.2 sec and produced a slightly crisper image of the seismicity. Finally, over 90% of the locations have estimates of epicentral and depth errors of 1 and 2 km respectively.

SEISMICITY OF SIERRA PIE DE PALO

Seismicity associated with Sierra Pie de Palo is mainly concentrated beneath the topographic limits of the mountain range, although there is a significant extension of activity just outside the southeast boundary of the range (Fig. 3). While the seismicity diminishes progressively to the east and south, it termi-nates rather abruptly along the northern and western limits of the mountain block. The center of mass of the seismicity beneath Sierra Pie de Palo from our data and previous local network studies is quite different from that obtained from teleseismic data. Teleseismic locations also show a concentration of activ-ity in the Sierra Pie de Palo area, but this activity is centered about 30 km to the east beneath the Bermejo Valley (Smalley and Isacks, 1990). A similar shift is observed for an m_b 5.3 event that occurred beneath the center of Sierra Pie de Palo and inside the network. The PDE location for this event is 30 km east of the location obtained using the local network data. The difference in location is probably best explained as the result of a systematic mislocation of events in this area by the worldwide network due to the relatively poor regional station coverage and use of an inappropriate velocity model.

In the map of Sierra Pie de Palo activity shown in Figure 3, events are shaded to indicate whether they are shallower or deeper than 20 km. This separates the seismicity pattern into two distinct nonoverlapping patterns representing shal-low and deep crustal seismicity. Two major trends are evident for the epicenters deeper than 20 km (light gray in Fig. 3). One trend is oriented north-northeast, parallel to the strike of the range, beneath the northern half of the mountain. The other shows a northwest-southeast alignment of epicenters across the southern part of the range, parallel to Sierra de Valle Fértil. Together these trends define the sharp western limit of the activity. To the east, the deep crustal seismicity terminates in a diffuse manner outside the borders of the southern half of the mountain block. In the northern part of the range, the deep crustal events are only found beneath the western side of the mountain block suggesting seismicity deepens to the west. Events shallower than 20 km (dark gray in Fig. 3) are concentrated in the eastern half of the mountain block. Their pattern suggests sets of along- and across-strike features. To the west and southwest of Sierra Pie de Palo, the activity is sparse and does not define any pattern. This activity, however, is thought to be in Sierras Pampeanas base-
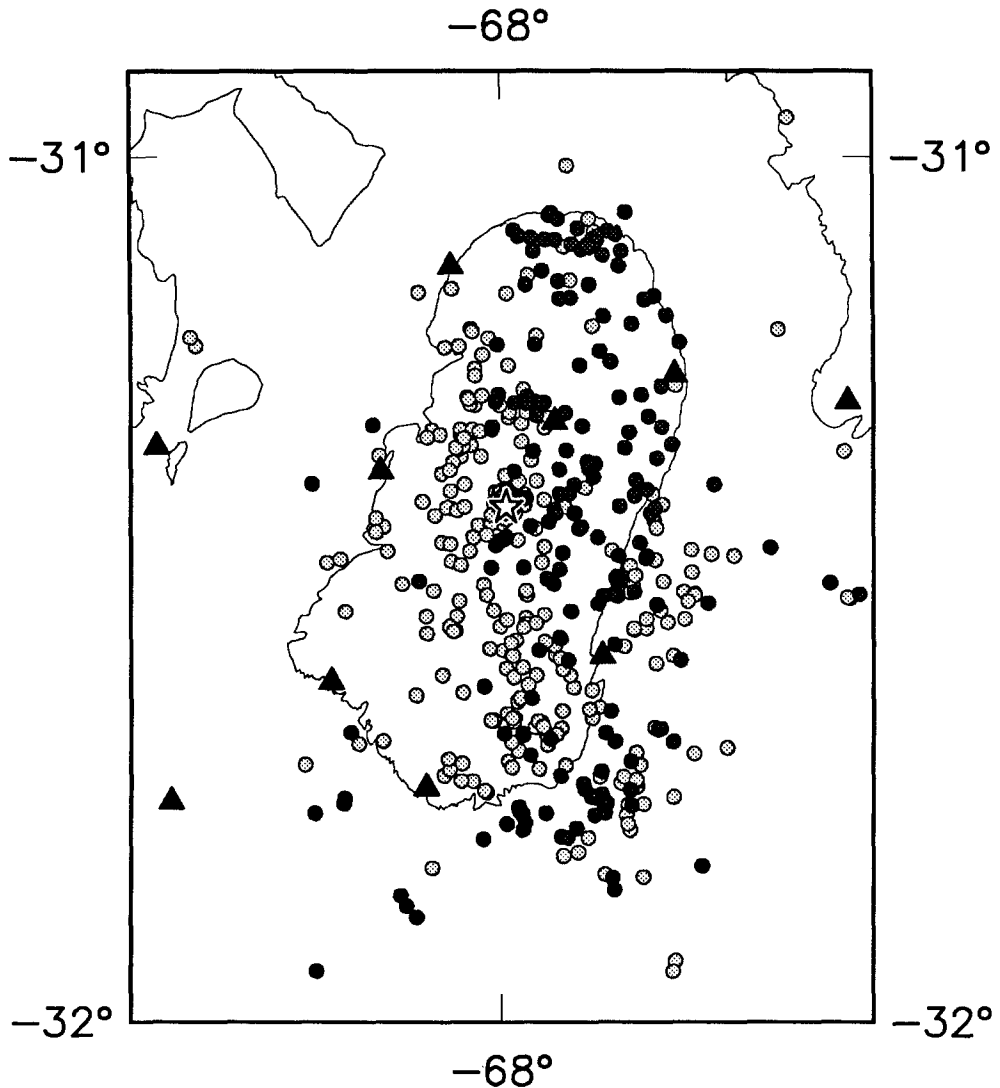
FIG. 3. Map of shallow epicenters (JHD locations). Approximately 600 shallow events are shown. Dark grey filled circles are events with depths shallower than 20 km; Light grey filled circles are events with depths between 20 and 40 km. Solid triangles are stations. The star is the epicenter of the m_b 5.3 event of 25 March 1988.

ment, since it is east of a line of small basement outcrops striking to the southwest from Sierra Pie de Palo (Smalley et al., 1992).

In a cross section oriented perpendicular to the trend of the range (Fig. 4a), the major features are (1) two east-dipping zones of seismicity, (2) a subhorizontal concentration of seismicity at 25-km depth, and (3) a large cluster of events with a volumetric distribution below the western side of the range. There are also suggestions of west-dipping alignments in the shallow activity beneath the west side of the range. A thick, west-dipping zone is also clear in an east–west-oriented cross section (Fig. 4b). The almost complete lack of activity in the southwestern part of the range (Fig. 3) suggests seismicity associated with a west-dipping fault is found primarily in the northern half of Sierra Pie de Palo.
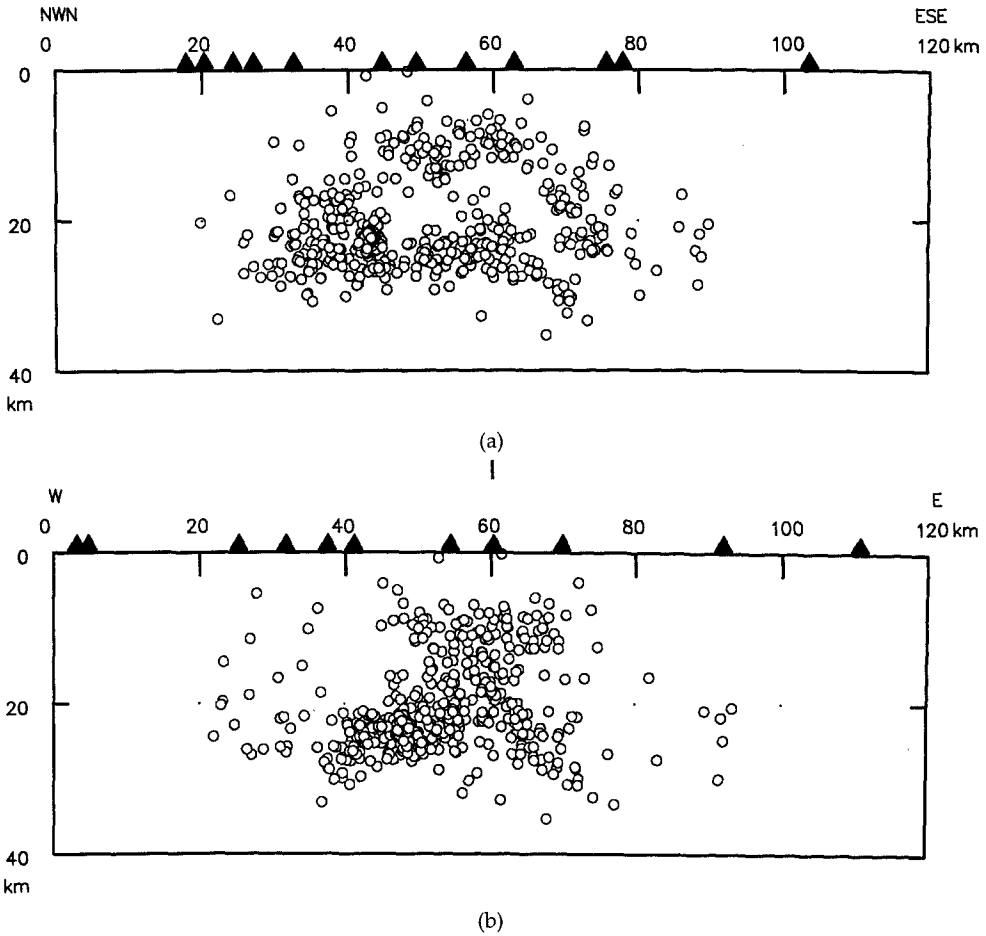
FIG. 4. Cross sections for shallow seismicity from Figure 3. (a) azimuth 115° and (b) azimuth 90°.

Two east-dipping planes in Figure 4a that partially overlap are subparallel in map view with along- and across-strike offsets. The southernmost of these planes is shifted eastward with respect to the other. These observations are consistent with a north-south variation of the seismicity and the associated major fault systems.

Focal mechanism solutions based on first-motion data were obtained using FOCMEC (Snoke *et al.*, 1984). This program does a grid search (a 5° grid in trend and plunge was chosen) to find all possible double couple solutions on the grid that are consistent with the first-motion data. A total of 120 single-event fault plane solutions were found using data recorded during a 5-month period, which we consider to be representative of the activity of Sierra Pie de Palo. We could not relate variations in focal plane orientation with depth because most of the focal mechanism solutions are from events deeper than 20 km. A major feature of the focal mechanism results is the lack of a spatially coherent pattern in either map view or depth distribution. As shown in Figure 5, the full range of fault types was found: thrust, normal, strike-slip, and oblique. Similar distributions of focal mechanism solutions have been observed in other areas, particularly after large earthquakes with complex rupture histories (Deschamp and

King, 1984; Oppenheimer, 1990). Roughly 60% of the data are thrust or reverse faults on roughly north–south-striking nodal planes (Fig. 5a), while mechanisms of the remaining events show a wide range of orientations (Fig. 5b).

To examine the regional stress field near Sierra Pie de Palo, the orientation of deviatoric stresses was computed by least-squares inversion of the focal mechanism data. The method proceeds in a grid search over the focal sphere, looking for the minimum of the sum of the squared misfit angles between the slip vectors and the direction of the shear stress resolved on the fault planes (Carey-Gailhardis and Mercier, 1987). This method implicitly assumes the stress field is homogeneous in the volume sampled. The best-fit maximum

(a)
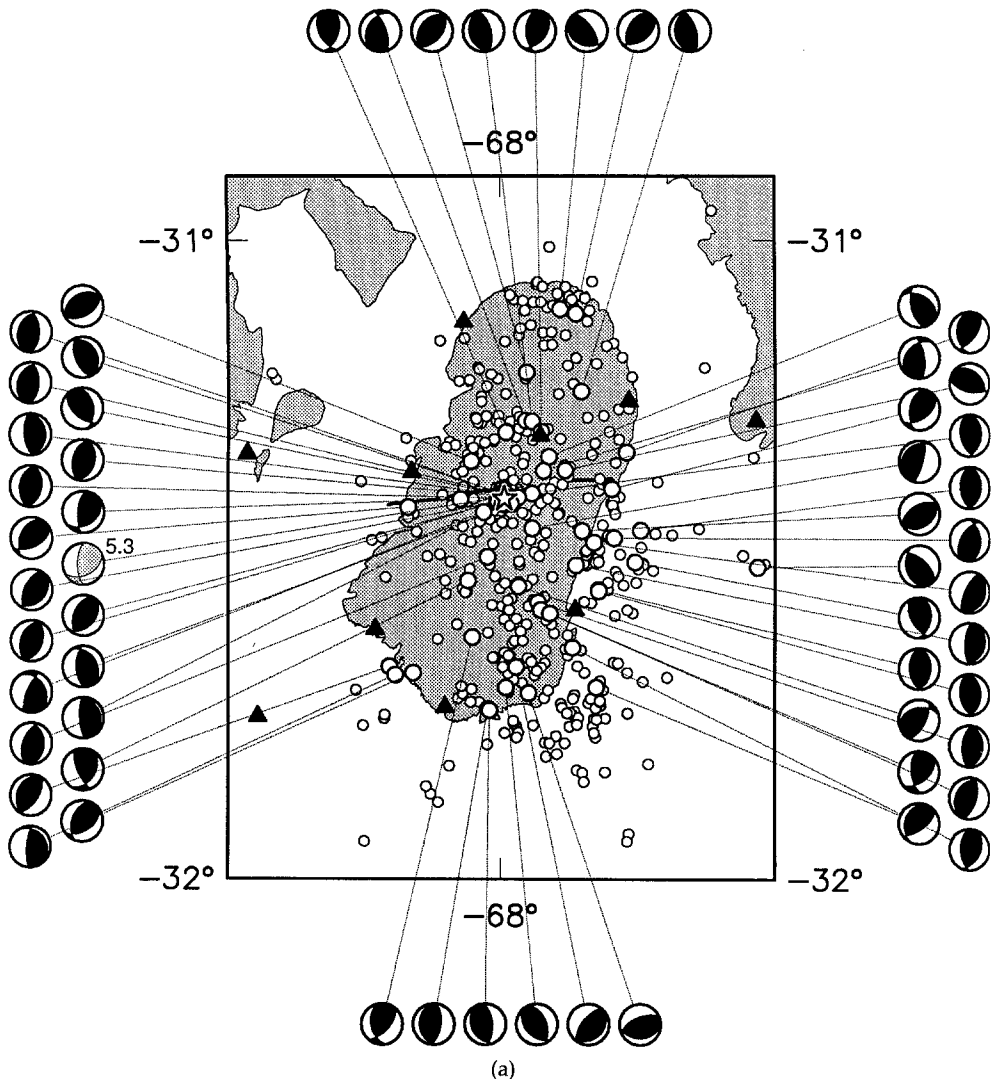
FIG. 5. Map of the seismicity with events having focal mechanism solutions identified by the larger circles. The mapped canyon (INPRES, 1977) cutting the range in two is also shown (solid bold line). (a) shows events with thrust and reverse fault-plane solutions, while (b) shows events with lateral and normal fault-plane solutions. Focal mechanism solutions are shown in upper hemisphere projections with compressional quadrants shaded black.

(b)
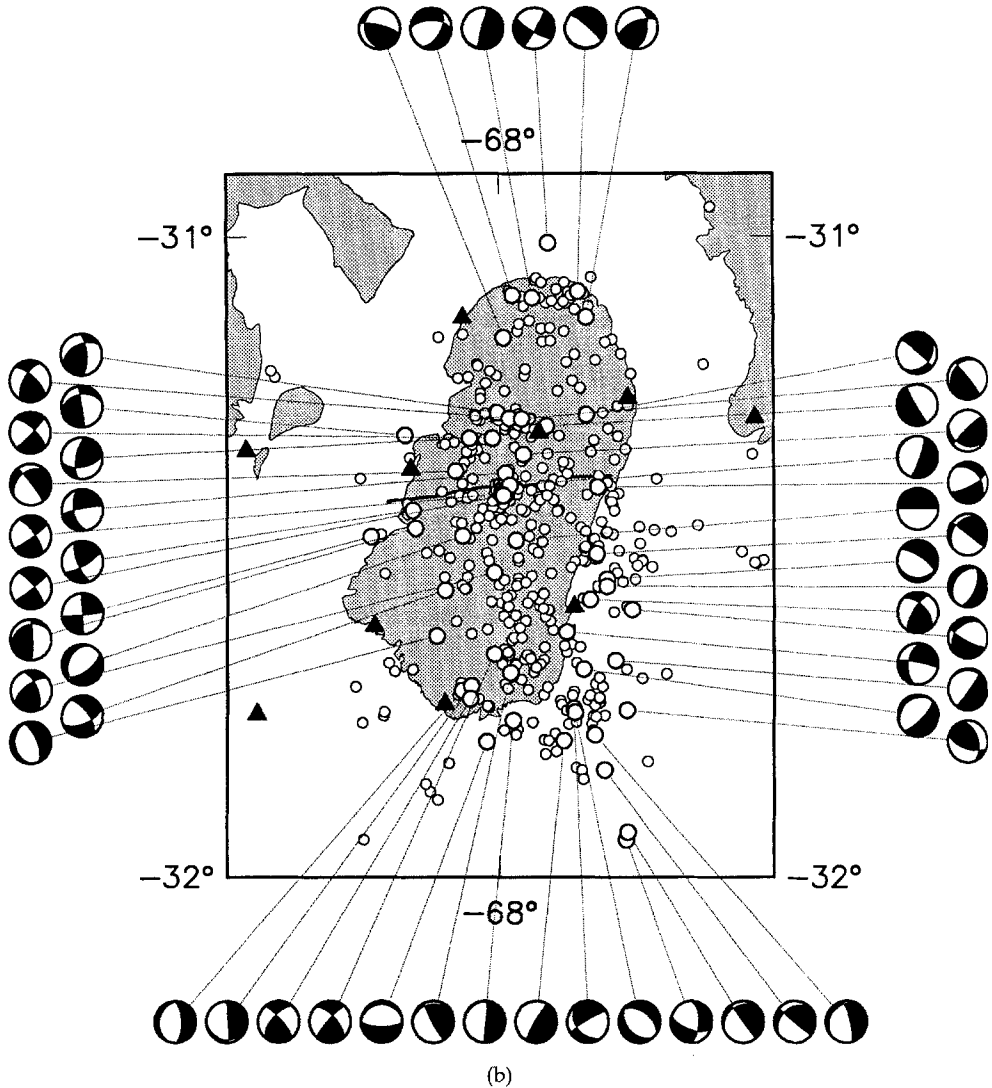
FIG. 5. (*Continued*).

compression axis, i.e., σ_1, is found to be at an azimuth of N107°E and a plunge of 13°. The corresponding minimum compression direction, σ_3, is at an azimuth of N120°W and a plunge of 72° (Fig. 6). The large value of the mean misfit angle (40°) indicates that this regional deviatoric stress tensor does not satisfactorily explain the data. The poor fit may be due to nonuniformity in the regional stress field, which violates the assumption of homogeneous stress implicit in the inversion method. With more focal mechanism solutions it may be possible to define subvolumes which meet the homogeneous stress requirement and obtain better results (Michael *et al.*, 1990). The results are, nevertheless, compatible with previous estimates of the regional stress directions obtained from studies of focal mechanisms of larger earthquakes (Stauder, 1975; Chinn and Isacks, 1983; Suarez *et al.*, 1983). The azimuth of σ_1, N107°E, is rotated 27° clockwise

azimuth   plunge

σ_1 axis :   107.31,   12.89

σ_3 axis :   240.80,   71.60

114 P & T axis plotted
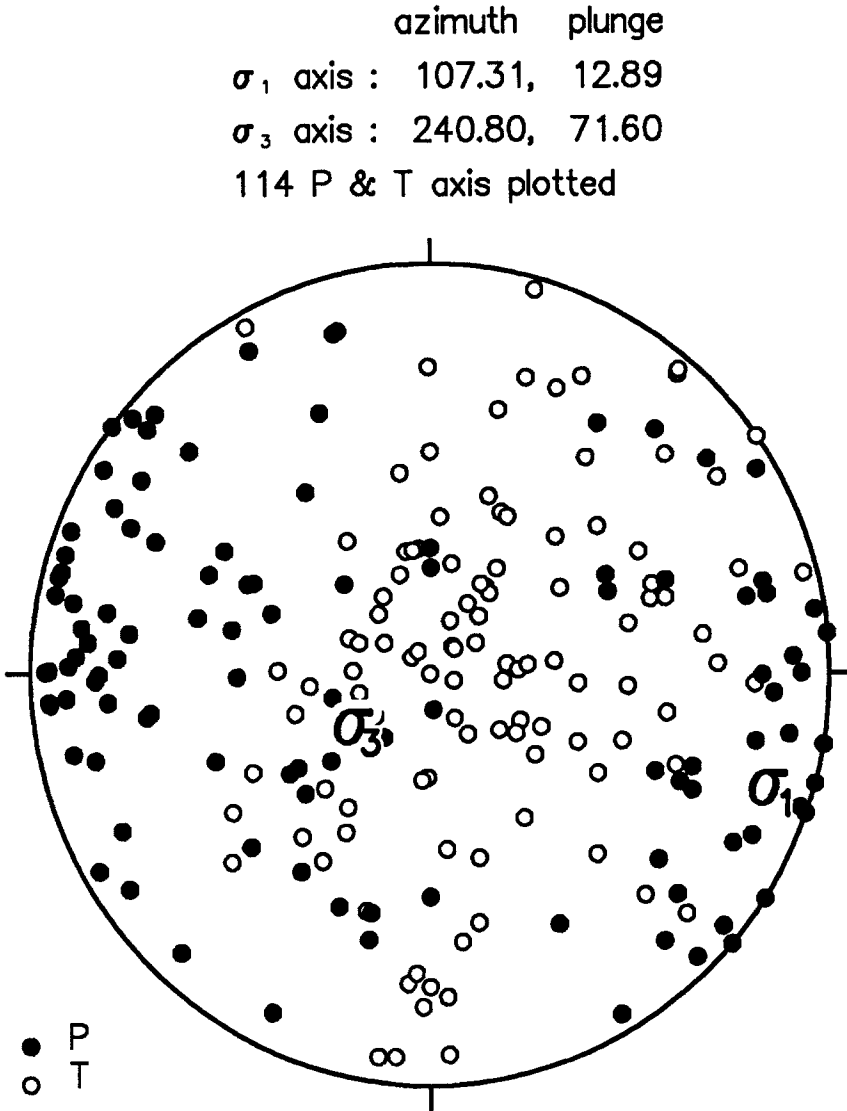
FIG. 6. Plot of the P (solid) and T (open circle) axis with result of inversion for the orientation of principal stresses $\sigma 1$ and $\sigma 3$. The scatter in P and T axes is quite large and may indicate the assumption of homogeneous stress does not apply for Sierra Pie de Palo.

from the plate convergence direction at the latitude of San Juan (DeMets *et al.*, 1990). This convergence direction, however, applies at the Nazca-South America plate boundary on the other side of the Andean orogen. The variation in direction must certainly reflect local variations in the stress field. Our result is consistent with a shortening direction perpendicular to the trend of Sierra Pie de Palo, and there may be a strong relationship between the shape of Sierra Pie de Palo and the regional stress field.

The difference between the convergence direction at the plate boundary and the maximum compressive stress direction in the Sierras Pampeanas could indicate a component of left-lateral strike-slip of imbricated lithospheric slivers

west of Sierra Pie de Palo. This would offset the central high Cordillera to the south relative to the Sierras Pampeanas. The situation here is similar to that of central Peru (Sébrier et al., 1988), which is also above a subhorizontally subducting segment. In this model, the Precordillera would be a zone of horizontal block rotations between the Sierras Pampeanas and High Cordillera Provinces.

The predominance of thrust and reverse mechanisms indicates Sierra Pie de Palo is under compression. The majority of mechanisms show east-southeast to west-northwest shortening perpendicular to the trend of Sierra Pie de Palo. The mechanisms are scattered uniformly through the seismicity and define a zone of thrust activity whose dimensions are on the order of the size of Sierra Pie de Palo. Some of the focal mechanisms have nodal planes striking northwest or northeast, indicating a nonuniform or perturbed stress field, which would be expected in a highly fractured source area. The m_b 5.3 event of 25 March 1988 has an oblique thrust mechanism with one plane striking north and the other striking N63°E and dipping 45°NW (Fig. 7). It also has a moderate strike-slip component that is not observed in the focal mechanism solutions for the Caucete earthquake or its aftershocks (Chinn and Isacks, 1983; Kadinsky-Cade, 1985). The small size of the rupture zone, on the order of a few square km for an earthquake of this magnitude, and the volumetric distribution of its aftershock sequence do not permit determination of the fault plane. The cluster of events around the m_b 5.3 event (Fig. 5a) for which focal mechanisms were obtained generally have thrust mechanisms and roughly define a northeast striking pattern. This suggests that the N63°E striking plane of the focal mechanism was the fault plane. The focal mechanism of the m_b 5.3 event indicates a dextral strike-slip component of crustal deformation. Such deformation is also suggested by the sheared grid pattern of epicenters observed in map view (Fig. 3). An alignment of strike-slip focal mechanisms along a very deep canyon that crust across Sierra Pie de Palo suggests right-lateral motion on vertical fault planes with horizontal, east-west, oriented P axis (Fig. 12). The canyon, which is a principal feature of Sierra Pie de Palo in LANDSAT images, has been eroded along a major ENE-WSW striking shear zone and practically cuts the range in two (INPRES, 1977). Geologic expression of such reverse or strike slip faults are also observed within other Pampean ranges (Jordan and Allmendinger, 1986). The shear zone leads to a natural division of the range into two zones whose seismicities are analyzed independently (Fig. 8). The boundary between the two groups of earthquakes is approximate and reflects the structural complexity of Sierra Pie de Palo, where several fault systems with different strike and dip orientations are inferred from the seismicity distribution as one crosses the range from north to south. The surface projections of the inferred fault plane from the m_b 5.3 earthquake and the alignment of events in the immediate area of the m_b 5.3 event also coincide with this major lineament of deformation.

Figures 9a and b show cross sections of all the events plus focal mechanism solutions of events with thrust and reverse faulting for the two zones defined in Figure 8. The strikes of the cross sections were selected to give the clearest image of planar features in the seismicity and they have unequal but subparallel strikes. The change in strike necessary for the cross-section views may imply a slight clockwise rotation of the local stress field as one goes from north to south. On the average, there is a good enough agreement between the dipping
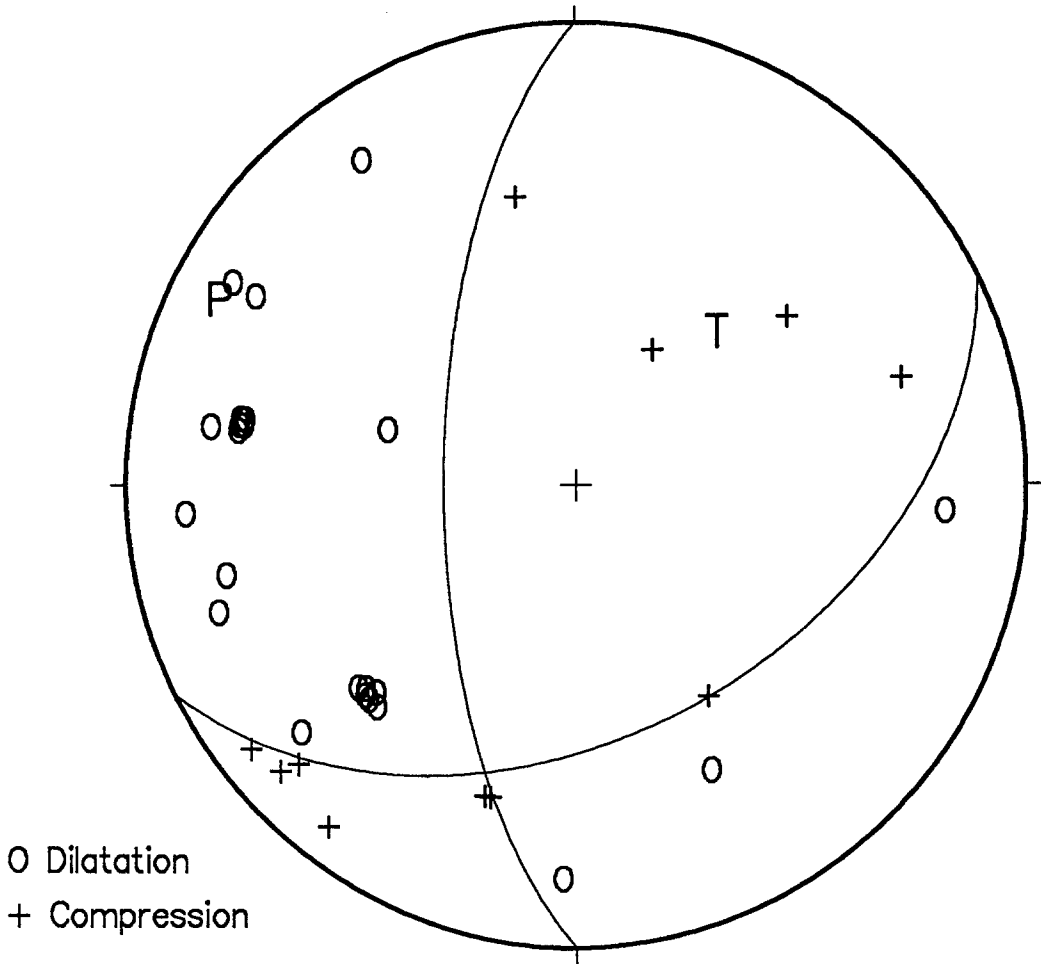
FIG. 7. Upper hemisphere, equal-area projection of fault plane solution for the m_b 5.3 event of 25 March 1988.

seismic zones in cross section and one of the nodal planes to interpret these features as buried thrust faults. There is a clear reversal of the dip direction of these seismicity patterns between the cross sections. The west-dipping seismic zone in the northern part (Fig. 9a) is quite thick and may be formed by a wide zone of deformation that includes several subparallel faults corresponding to the layering of epicenters observed in cross section. Alternatively, the thickness can reflect the concentration of stress on a thrust fault locked by listric curvature. A plane fit through the mean of the data intersects the surface east of the range in the Bermejo Valley, where there is no surficial evidence of deformation. The slight listric bend observed along the lower boundary of the seismicity and the sharp termination of the seismicity beneath the eastern side of the range (Fig. 8) are consistent with the presence of a curved fault, whose dip increases near the surface. The thickness of the thrust zone and the presence of events in the hanging wall block (Fig. 9a) could be the result of space problems created by curvature of the fault. In the very dense cluster of activity near 25 km depth, events that have focal mechanism solutions tend to align perpendicular to the
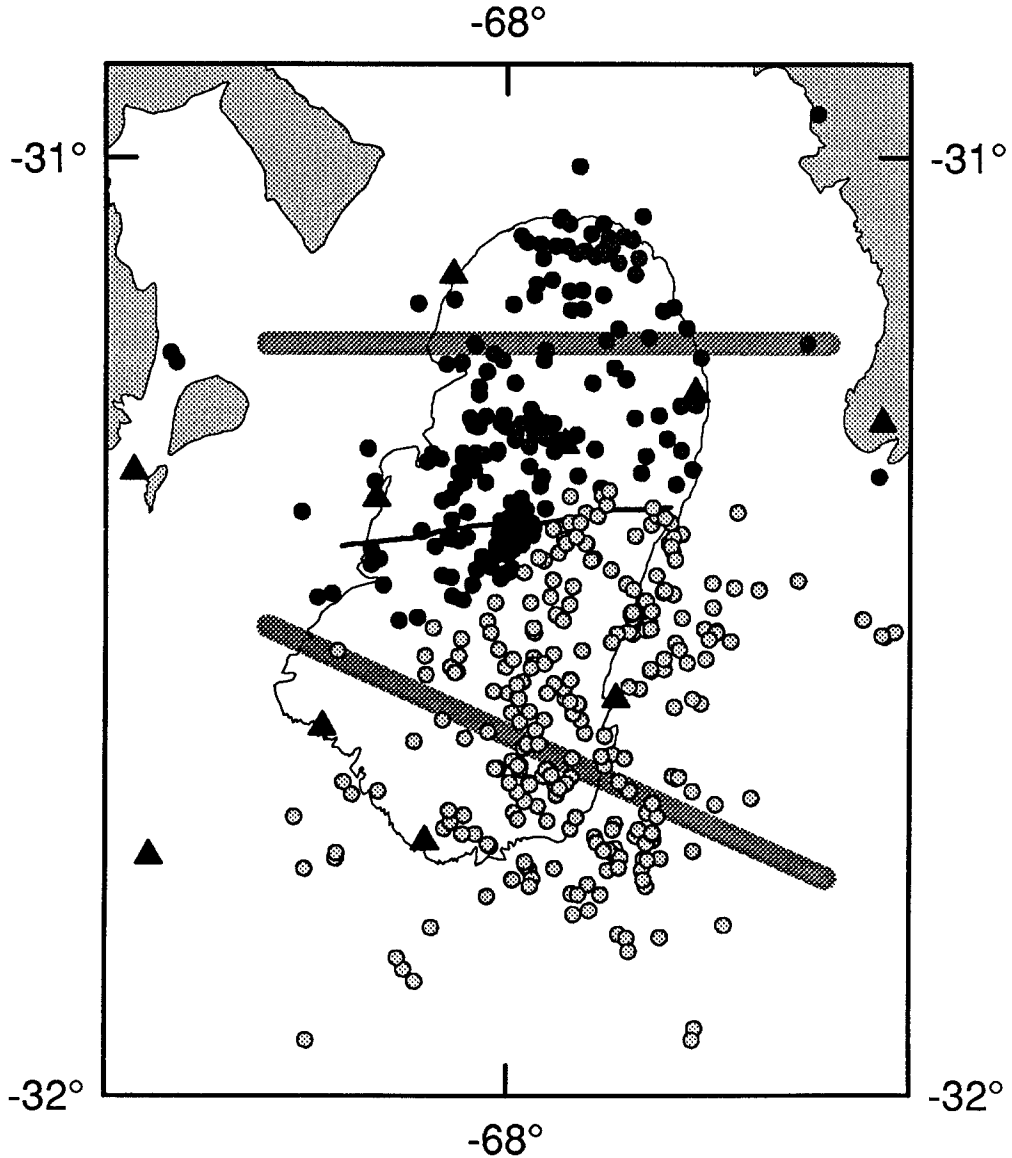
FIG. 8. Map of the two zones of seismicity used to construct the cross sections of Figure 9. The cross sections do not have a fixed width in map view as only the selected events are projected. The contact between the two zones approximately follows a deep canyon that cuts diagonally across the center of the range.

thrust zone. Their focal mechanisms indicate thrust motion in which one plane is coincident with the subvertical east-dipping alignment of hypocenters. They might represent conjugate or antithetic faulting needed to accommodate the local space problems induced by the fault curvature.

In the southern segment of two east-southeast-dipping planes (Fig. 9b) in the seismicity project to the surface on the western slope of Sierra Pie de Palo in the highly deformed central part of the range. As in the northern segment, there are no mapped surface faults corresponding to the surface intercepts. The lack of
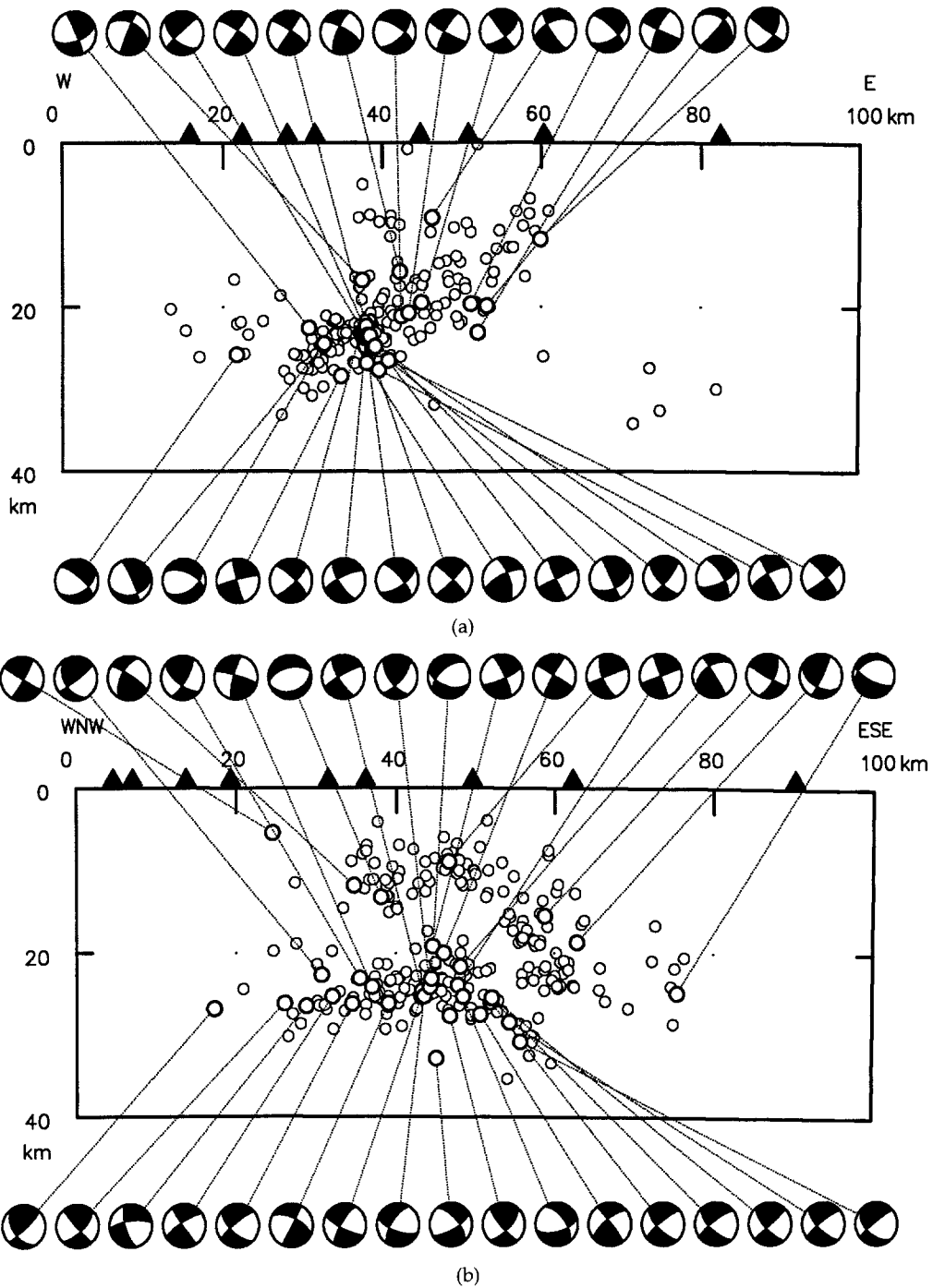
FIG. 9. One-to-one cross sections of seismicity (a) for the northern block (dark grey filled circles on Fig. 8) and (b) for the southern block (light grey filled circles on Fig. 8).

seismicity shallower than 7 km in this figure may be an artifact of the location process or due to a decrease in overall stress levels as the free surface is approached. Another feature of the cross section is the triangle-shaped cluster of activity bounded on the east by the deeper of the east-dipping thrust faults and on the bottom by a nearly flat base at 27-km depth. Despite the well-defined boundaries, no clear alignments can be seen in this group of hypocenters, indicating that the strike of the activity is not perpendicular to the cross section (azimuth N115°E) or the activity is not associated with a planar structure. Several focal mechanisms in this cluster of activity indicate east-west thrusting, but their nodal planes do not line up with the subhorizontal trend of the seismicity. The focal mechanisms and geometry suggest a complex interaction between the sheared zone and the east-dipping fault rather than a simple thrust fault. This model is also supported by a thickening of the cluster from west to east. The average depth here is similar to the maximum depth found in the west-dipping seismic zone in the northern segment (Fig. 9a). The northern and southern zones merge near the epicenter of the m_b 5.3 event and are inseparable in map view (Fig. 3). The division of the range by the sub-vertical shear zone allows the major faults in the northern and southern parts of the range to have different dips, although they both terminate into a large subhorizontal shear zone at about 30-km depth (Fig. 10).

A cross section oriented along the strike of Sierra Pie de Palo (N23°E) (Fig. 11) shows most of the activity is deeper than 20 km. Seismicity terminates abruptly at the northern end of Sierra Pie de Palo in a subvertical alignment of events, one of which has a strike-slip focal mechanism solution. The depth of this vertical cluster reaches a depth of 32 km, suggesting that a crustal scale oblique strike-slip fault terminates the north end of Sierra Pie de Palo. There is virtually no shallow earthquake activity north of this limit in the area covered by the network. While the eastern Precordillera seismicity pattern is dramatically different (Smalley *et al.*, 1992), it also ends abruptly at the same
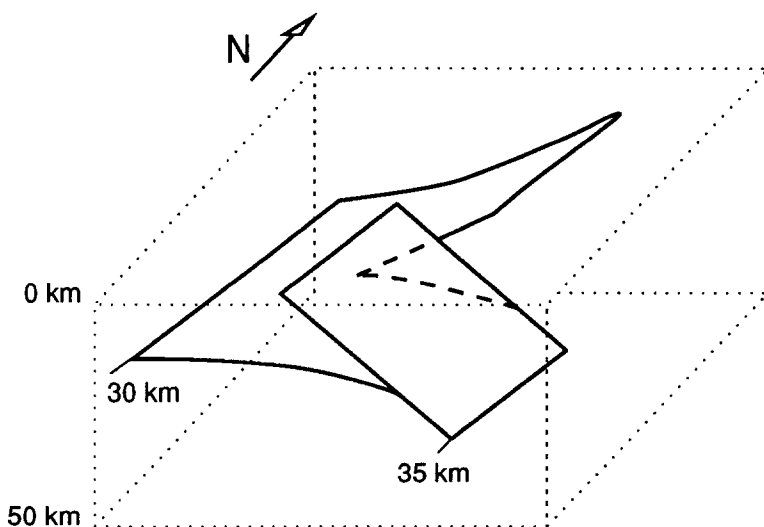
FIG. 10. Schematic three-dimensional perspective views of the fault geometry inferred from the spatial distribution of the seismicity.
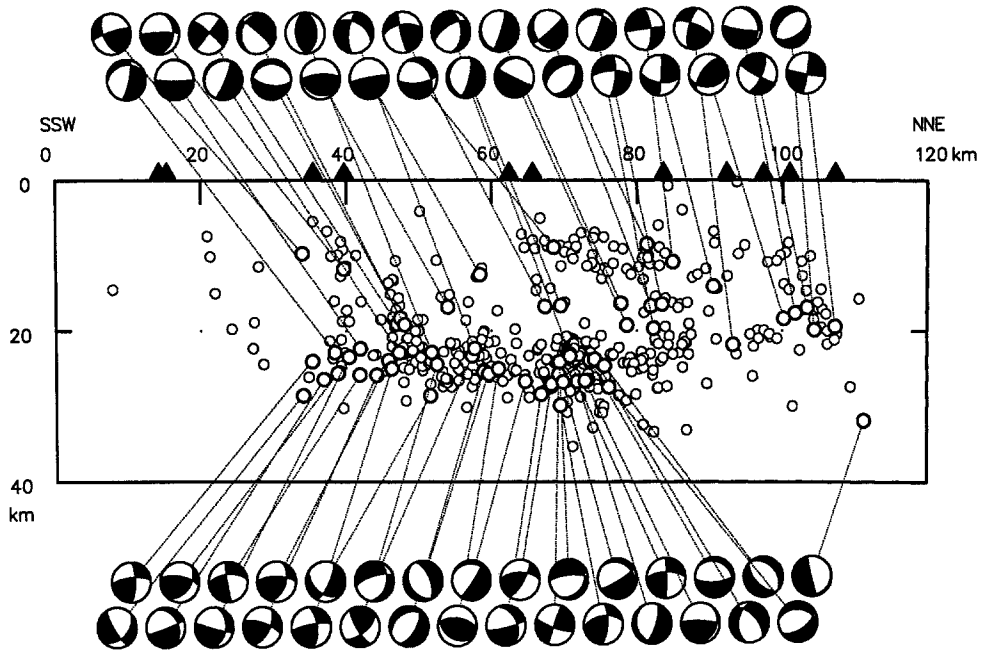
FIG. 11. Cross section striking N23°E, parallel to the trend of Sierra Pie de Palo. Seismic activity around 25-km depth runs beneath the entire structure but does not extend beyond the topographic limits of the mountain range.

latitude (31°S) as the Sierra Pie de Palo activity. This change in seismic activity may be associated with a regional tectonic boundary that crosses both the Sierras Pampeanas and Precordillera terranes. This boundary is expressed by a large change to the depth of basement immediately north of Pie de Palo, where the Bermejo Valley is filled with at least 6 km of Cenozoic strata on the western side and probably more on the eastern side (Fielding and Jordan, 1988). The southern termination of activity is also relatively sharp and occurs in a cluster beneath the southeast corner of the range. This activity forms at least two clear subvertical planes that extend from a depth of 10 km to more than 30 km along an east-southeast trend perpendicular to the strike of the range (Figs. 3 and 8). The seismicity concentrated in the layer between 25- to 30-km depth exhibits a complex pattern of short, 5- to 10-km, moderately northward- or southward-dipping lineations, indicating a complex faulting. This interpretation is supported by the wide variety of focal mechanisms observed along-strike throughout the range.

DISCUSSION

We conducted a microseismic study in the Sierras Pampeanas tectonic province of the Andean foreland to investigate the mechanism responsible for the uplift of the Sierras Pampeanas mountain blocks. The Sierras Pampeanas occur in an area of the foreland over a region where the Nazca Plate, as defined by the Wadati-Benioff zone, is subducting subhorizontally. Although the individual ranges of the Sierras Pampeanas may all be the result of similar tectonic processes, on the time scale of our temporary network and modern seismology they have very different levels of seismic activity. Seismicity associated with the

Pampean province is notable in the PDE and ISC catalogs. Except for the high level of activity associated with Sierra Pie de Palo, however, the activity level throughout the rest of the province is rather low. Interestingly, Sierra Pie de Palo is the only Pampean range to have experienced a major earthquake in the recent past. Does this indicate the present activity associated with Sierra Pie de Palo is still part of a long-term aftershock sequence, 10 years after the 1977 M_s 7.3 Caucete earthquake mainshock? By comparison, very few earthquakes were recorded from the nearby Pampean range Sierra de Valle Fértil even though the network was capable of recording events there (two stations were even located on Sierra de Valle Fértil). This observation confirms the differences in seismicity level noted from teleseismic data.

Crustal seismicity beneath Sierra Pie de Palo shows that the crustal material there is highly fractured and has several very active fault systems. The wide variety of focal mechanisms also indicates a highly nonuniform stress field. The Caucete event was modeled by Kadinsky-Cade (1985) as a complex double shock whose component shocks were separated in time and space by 20 sec and 64 km, respectively. It is likely that fault slip during the double shock was no uniform, and, as the rupture did not reach the surface, large variations in slip and stress must exist around the boundary of the fault planes. Several studies have shown that aftershocks tend to cluster off the principal rupture surface as a result of the redistribution of stress by the mainshock and therefore do not always occur where the slip during the mainshock was the greatest (Doser and Kanamori, 1986; Mendoza and Hartzell, 1988). Chinn and Isacks (1983) found the depth of the Caucete event to be 17 km using a technique based on the comparison of synthetic and observed seismograms. In the seismicity recorded by our temporary network, no significant activity is found at this depth (Fig. 4), suggesting a relative decrease in stress around the region of the focus after the mainshock. The highly variable stress field generated by the mainshock, together with the complicated block geometry of the range, could explain the variety of focal solutions (Oppenheimer, 1990) and the scattered pattern of seismicity associated with Sierra Pie de Palo. Similarities in the seismicity patterns defined in this study, the activity of 1980 and 1984/5 (Smalley and Isacks, 1990), and the Caucete earthquake aftershocks (Langer and Bollinger, 1988) support a model of a long-lasting aftershock sequence for the Caucete earthquake. It is very possible that the unusual seismicity level of Sierra Pie de Palo now is attributable to the 1977 Caucete event.

The focal mechanism of the Caucete earthquake (Chinn and Isacks, 1983; Kadinsky-Cade, 1985) is a pure thrust with approximately north–south-striking nodal planes. The traditional question regarding selection of the fault plane from the two nodal planes continues to cause controversy in the interpretation of this event. Neither the aftershock study nor modeling of the coseismic deformation (Kadinsky-Cade and Reilinger, 1985; Langer and Bollinger, 1988) can unambiguously determine whether the event occurred on the east- or west-dipping plane. Aftershock data (Langer and Bollinger, 1988), collected during an 11-day period starting about 2 weeks after the mainshock, show an X pattern similar to that found in our data in Figure 4b, but the low resolution of the aftershock data set could not answer the question of the dip direction of the mainshock, nor resolve the two planes individually. Geodetic measurements have also been modeled successfully for both east- (Langer and Bollinger, 1988) and west-dipping faults (Kadinsky-Cade and Reilinger, 1985), which is not

surprising considering the known nonuniqueness of the inversion of such data. The very good spatial resolution we achieved, however, still does not provide a simple answer to the question of finding the orientation of the dip of the Caucete earthquake fault. If the activity associated with the m_b 5.3 event is removed, the remaining data set has approximately the same number of events in the east- and west-dipping zones, precluding a choice based on the largest population.

Our data do, however, suggest a solution to the problem of the fault orientation of the Caucete event. The division of Sierra Pie de Palo into two distinct zones (northern and southern, see Fig. 8) suggests that the two shocks of the Caucete event may have occurred on different fault planes, one associated with each zone. This supports the idea that Sierra Pie de Palo is not acting as a single block, but as two distinct blocks with some sort of transfer structure between them. The reversal of dip between the two fault planes observed in our data, or the X pattern from the aftershock data, suggests the two events that make up the Caucete earthquake occurred on two faults with opposite dips.

Aftershock activity often delineates a planar structure coinciding with the mainshock fault plane. It can also be distributed along nearby subsidiary or secondary faults as in the case of the Loma Prieta earthquake. In Loma Prieta, aftershock activity was found on both the San Andreas and Sargent faults, while the mainshock was on the San Andreas fault only (Dietz and Ellsworth, 1990). A single fault model for the Caucete event is possible if the aftershocks and continuing activity are on a conjugate set of east dipping faults and the main fault. The dense concentration of seismicity at 25 km depth is difficult to integrate into this model. In models with two faults dipping in opposite directions, the subhorizontal seismic plane may represent a mid-crustal shear zone or décollement that connects the two thrust faults (Fig. 10).

The topography of Sierra Pie de Palo also supports a model with multiple faults beneath the range since it does not have the shape expected for a mountain built up by successive throw along a single thrust fault, as is the case for Sierra de Valle Fértil (Fielding and Jordan, 1988). It suggests a more complex deformation involving several sets of faults most likely based on reactivation of pre-existing faults. As noted in studies of LANDSAT images (Jordan and Allmendinger, 1986), the crest of Sierra Pie de Palo is not a straight line but bends southwesterly as it crosses the canyon, suggesting that the range is sheared in a right-lateral sense across the canyon. The highest elevations (maximum 3 km) also occur on the north side of the canyon. Almost all the strike-slip mechanisms we found also show right lateral motion on northeast-trending faults (Fig. 12). Their epicenters are distributed along the range but also along the canyon and immediately north of it, supporting the interpretation that the central part of Sierra Pie de Palo is the locus of a northeast-striking, right-lateral deformation. The strike-slip events along the southern limit of seismicity can be related to the termination of the thrust fault in the south. These mechanisms represent adjustments of the medium to the decrease of slip near the edge of the faulting. The inferred northeast orientation of right-lateral deformation is rotated more than 30° counterclockwise from the direction of maximum compression (N107°E), which is larger what would be expected for Coulomb failure, suggesting that the strike-slip motion is occurring on a pre-existing northeast structure. Such a structure on a regional scale is seen in LANDSAT images where it is expressed as a 300-km-long,
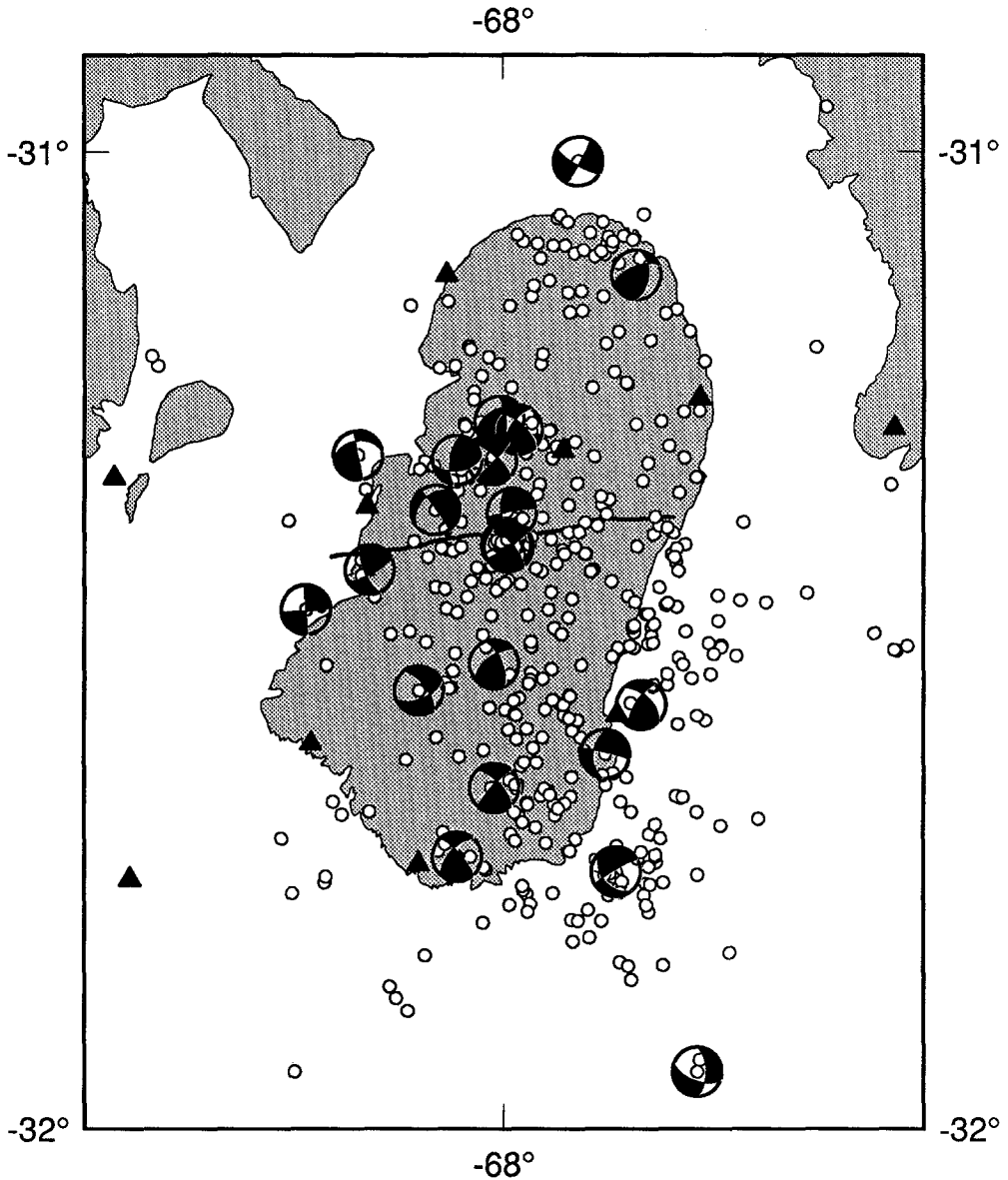
FIG. 12. Map of strike slip-fault plane solutions. Several of them roughly follow the canyon, which is the surface trace of the inferred limit between the two blocks defined by the seismicity.

northeast-trending lineament exhibiting apparent right-lateral offset. This lineament cuts across the center of Sierra Pie de Palo, is coincident with a change in the structure of Sierra de Valle Fértil, and continues to the east, outside the immediate area of our study, for at least 100 km (Jordan and Allmendinger, 1986).

CONCLUSIONS

The increased resolution and quality of our data provide a significantly improved view of the seismicity of the Sierra Pie de Palo area. The concentration of seismicity and the level of activity associated with Sierra Pie de Palo

compared with the relative quiescence of the neighboring mountain blocks suggests that the present seismicity near Pie de Palo is part of an ongoing aftershock sequence of the M_s 7.3 Caucete earthquake that occurred there in 1977. Ten years later, this activity still presents an opportunity to infer some characteristics of the 1977 event. In particular, the seismicity pattern of the mountain is divided into two parts (northern and southern blocks). The sepratrix between these blocks is coincident with a major shear zone crossing the mountain that is expressed as a deeply eroded canyon. Distinct, though complex, systems of faults were resolved in both the northern and southern blocks. A model for the Caucete earthquake with sequential failure of faults in both blocks can address several observations and controversies about this earthquake. First, the earthquake is known to be a double shock. It is thought to have initiated with a magnitude M_s 6.8 foreshock (Kadinsky-Cade, 1985) in the northern part of the range (the ISC location for the event). The foreshock triggered the magnitude M_s 7.3 mainshock, with an epicenter of 64 km south of and 20 sec later than the foreshock, in the southern block (Kadinsky-Cade, 1985). Earlier studies found a roughly X-shaped feature in cross section but were unable to resolve it into separate faults in map view. Our data image a seismically defined west-dipping fault plane in the north and an east-dipping fault plane in the south. The volumetric aspect of the seismicity also suggests the presence of numerous antithetic faults. The division of the range into northern and southern blocks across a right-lateral shear zone is supported by a concentration of focal mechanism solutions along the shear zone showing the right-lateral strike-slip motion and by regional scale strike-slip faults identified on satellite images. The orientation of the local stress field obtained from inversion of P- and T-axis data is oriented N107°E. This is notably different from the Nazca-South America plate convergence direction of N79°E (DeMets et al., 1990). This might be due to local boundary effects between blocks inside the Sierras Pampeanas Province and/or stress redistribution of a component of the regional tectonic stresses relieved by the mainshock. The variety of aftershock mechanisms indicates that many events occurred on pre-existing faults and demonstrates the complexity of faulting that can follow a large earthquake. Another explanation of the discrepancy between plate convergence direction and orientation of maximum stress from these data could be the presence of a component of sinistral strike-slip motion west of the Sierras Pampeanas. The clustering of seismicity directly beneath the range and almost completely within its topographic limits and the quiescence of the neighboring intermontane valley suggests that brittle crustal deformation here is concentrated in the immediate region of the individual mountain blocks and is not found uniformly or continuously throughout the Pampeanas Province. There is also no topographic indication of large scale thickening of the lower ductile crust under the Sierras Pampeanas Province (Isacks, 1988). Crustal thickening associated with isostatic compensation may occur locally, producing a Moho with topography that is roughly a mirror image of the surface topography rather than a relatively smooth but deeper Moho implying a thickened crust on a regional scale.

REFERENCES

Baranzangi, M. and B. Isacks (1976). Spatial distribution of earthquakes and subduction of the Nazca plate beneath South America, *Geology* **4**, 686–692.

Baranzangi, M. and B. Isacks (1979). Subduction of the Nazca plate beneath Peru: evidence from spatial distribution of earthquakes, *Geophys. J.* **57**, 537–555.

Bollinger, G. A. and C. J. Langer (1988). Development of a velocity model for locating aftershocks in the Sierra Pie de Palo region of western Argentina, *USGS Bull. 1795*.

Caminos, R., C. A. Cingolani, F. Hervé, and Eastern Linares (1982). Geochronology of the pre-Andean metamorphism and magmatism in the Andean Cordillera between latitudes 30° and 36°S, *Earth Sci. Rev.* **18**, 253–283.

Carey-Gailhardis, E. and J. L. Mercier (1987). A numerical method for determining the state of stress using focal mechanisms of earthquake populations: application to Tibetan teleseisms and microseismicity of Southern Peru, *Earth Planet. Sci. Lett.* **82**, 165–179.

Chinn, D. S. and B. L. Isacks (1983). Accurate source depths and focal mechanisms of shallow earthquakes in western South America and in the New Hebrides Island Arc, *Tectonics* **2**, 529–563.

Chiu, J. M., G. C. Steiner, R. Smalley, Jr., and A. C. Johnston (1991). The PANDA seismic array: a simple, working system, *Bull. Seism. Soc. Am.* **81**, 1000–1014.

DeMets, C., R. G. Gordon, D. F. Argus, and S. Stein (1990). Current plate motions, *Geophys. J. Int.* **101**, 425–478.

Deschamp, A. and G. C. P. King (1984). Aftershocks of the Campania-Lucania (Italy) earthquake of 23 November 1980, *Bull. Seism. Soc. Am.* **74**, 2483–2517.

Dietz, L. D. and W. L. Ellsworth (1990). The October 17, 1989, Loma Prieta, California, earthquake and its aftershocks: geometry of the sequence from high-resolution locations, *Geophys. Res. Lett.* **17**, 1417–1420.

Dorbath, C., L. Dorbath, A. Cisternas, J. Deverchère, M. Diament, L. Ocola, and M. Morales (1986). On crustal seismicity of the amazonian foothill of the central Peruvian Andes, *Geophys. Res. Lett.* **13**, 1023–1026.

Doser, D. I. and H. Kanamori (1986). Depth of seismicity in the Imperial Valley region (1977–1983) and its relationship to heat flow, crustal structure, and the October 15, 1979, earthquake, *J. Geophys. Res.* **91**, 675–688.

Fielding, E. J. and T. E. Jordan (1988). Active deformation at the boundary between the Precordillera and Sierras Pampeanas, Argentina, and comparison with ancient Rocky Mountain deformation, in *Rocky Mountain Foreland and the Cordilleran Thrust Belt*, W. J. Perry and C. J. Schmidt (Editors) *Geol. Soc. Am. Memoir* **171**, 143–163.

Frohlich, C. (1979). An efficient method for joint hypocenter determination for large groups of earthquakes, *Computers and Geosciences* **5**, 387–389.

INPRES (Instituto Nacional de Prevención Sísmica) (1977). El terremoto de San Juan del 23 de Noviembre de 1977, Informe Preliminar, República Argentina, San Juan, 103 pp.

Isacks, B. L. (1988). Uplift of the central Andean Plateau and bending of the Bolivian Orocline, *J. Geophys. Res.* **93**, 3211–3231.

Isacks, B. L. and M. Barazangi (1977). Geometry of Benioff zones: Lateral segmentation and downward bending of the subducted lithosphere, in Island Arcs, Deep Sea Trenches, and Back-Arc Basins, Maurice Ewing Ser., vol. 1, edited by M. Talwani and W. C. Pitman III, pp. 99–114, AGU, Washington, D.C.

Jordan, T. E. and R. W. Allmendinger (1986). The Sierras Pampeanas of Argentina: A modern analogue of Rocky Mountain foreland deformation, *Am. J. Sci.* **286**, 737–764.

Jordan, T. E., B. Isacks, R. Allmendinger, J. Brewer, V. Ramos, and C. Ando (1983). Andean tectonics related to geometry of subducted Nazca plate, *Geol. Soc. Am. Bull.* **94**, 341–361.

Kadinsky-Cade, K. (1985). Seismotectonics of the Chile margin and the 1977 Caucete earthquake of western Argentina, *Ph.D. Thesis*, Cornell University, Ithaca, New York.

Kadinsky-Cade, K. and R. Reilinger (1985). Surface deformation associated with the November 23, 1977, Caucete, Argentina earthquake sequence, *J. Geophys. Res.* **90**, B14, 12691–12700.

Klein, F. W. (1978). *Hypocenter Location Program HYPOINVERSE. Part 1. Users guide to versions 1, 2, 3, and 4,* U.S. Geol. Surv. Open-File Rep. 78–694.

Langer, C. J. and G. A. Bollinger (1988). Aftershocks of the western Argentina (Caucete) earthquake of 23 November 1977: some tectonic implications, *Tectonophysics* **148,** 131–146.

Mendoza, C. and S. H. Hartzell (1988). Aftershocks patterns and main shock faulting, *Bull. Seism. Soc. Am.* **78,** 1438–1449.

Michael, A. J., W. L. Ellsworth, and D. H. Oppenheimer (1990). Coseismic stress changes induced by the 1989 Loma Prieta, California earthquake, *Geophys. Res. Lett.* **17,** 1441–1444.

Oppenheimer, D. H. (1990). Aftershock slip behavior of the 1989 Loma Prieta, California earthquake, *Geophys. Res. Lett.* **17,** 1199–1202.

Regnier, M., R. Smalley, J. M. Chiu, D. Vlasity, J. Pujol, A. Johnston, G. Steiner, J. Bollwerk, J. Vlasity, B. Isacks, T. Cahill, D. Whitman, J. L. Chatelain, F. Bondoux, J. Castano, and N. Puebla (1988). Analysis of an m_b 5.3 earthquake and its aftershocks sequence in the thick-skinned Pampeanas of the Andean foreland, *EOS* **69,** 1316.

Salfity, J. A. and S. Gorustovich (1983). Paleogeografía de la cuenca del grupo Paganzo (Paleozoico Superior), *Asoc. Geol. Argent. Rev.* **38,** 437–453.

Sebrier, M., J. L. Mercier, J. Macharé, D. Bonnot, J. Cabrera, and J. L. Blanc (1988). The state of stress in an overriding plate situated above a flat slab: the Andes of central Peru, *Tectonics* **7,** 895–928.

Sebrier, M., J. L. Mercier, F. Mégard, G. Laubacher, and E. Carey-Gailhardis (1985). Quaternary normal and reverse faulting and the state of stress in the central Andres of south Peru, *Tectonics* **4,** 739–780.

Smalley, R., Jr. and B. L. Isacks (1990). Seismotectonics of thin and thick-skinned deformation in the Andean foreland from local network data: evidence for a seismogenic lower crust, *J. Geophys. Res.* **95,** 12487–112498.

Smalley, R., Jr., J. Pujol, M. Regnier, J. M. Chiu, B. L. Isacks, M. Araujo, and N. Puebla (1992). Basement seismicity beneath the Andean Precordillera thin-skinned thrust belt and its implications for crustal and lithospheric behavior (submitted for publication).

Snoke, J. A., J. W. Munsey, and G. A. Bollinger (1984). A program for focal mechanism determination by combined use of polarity and SV-P amplitude ratio data (abstract), *Earthquake Notes* **55,** No. 3, 15.

Stauder, W. (1973). Mechanism and spatial distribution of Chilean earthquakes with relation to subduction of the oceanic plate, *J. Geophys. Res.* **78,** 5033–5061.

Stauder, W. (1975). Subduction of the Nazca plate under Peru as evidenced by focal mechanisms and by seismicity, *J. Geophys. Res.* **80,** 1053–1064.

Suárez, G., J. Gagnepain, A. Cisternas, D. Hatzfeld, P. Molnar, L. Ocola, S. W. Roecker, and J. P. Viodé (1990). Tectonic deformation of the Andes and the configuration of the subducted slab in Peru: results from a microseismic experiment, *Geophys. J. Int.* **103,** 1–12.

Suárez, G., P. Molnar, and B. C. Burchfiel (1983). Seismicity, fault plane solutions, depth of faulting and active tectonics of the Andes of Peru, Ecuador, and southern Columbia, *J. Geophys. Res.* **88,** 10403–10428.

Vlasity, D. (1988). A crustal seismicity study in the San Juan, Argentina region using digital seismograms collected by the Panda Array, *M.S. Thesis,* Memphis State University, Memphis, Tennessee.

Volponi, F. S. (1968). Los terremotos de Mendoza del 21 de Octubre de 1968 y la estructura de la corteza terrestre, in *Acta Cuyana de Ingeniería,* XII, San Juan, Argentina, Instituto Sismológico Zonda, Facultad de Ingeniería, Universidad Nacional de Cuyo, 95–110.

INSTITUTE FRANÇAIS DE RECHERCHE
SCIENTIFIQUE POUR LE
DÉVELOPPEMENT EN COOPERATION
NOUMEA, NEW CALEDONIA
  (M.R., J.L.C.)

INSTITUTE FOR THE STUDY OF
THE CONTINENTS
CORNELL UNIVERSITY
ITHACA, NEW YORK 00000
  (B.L.I.)

CENTER FOR EARTHQUAKE RESEARCH AND INFORMATION
MEMPHIS STATE UNIVERSITY
MEMPHIS, TENNESSEE 00000
  (R.S., J.-M.C.)

INSTITUTO NACIONAL DE PREVENCIÓN SÍMICA
SAN JUAN, ARGENTINA
  (M.A.)